Diagnosing subseasonal and seasonal drivers of European and North African winter extremes using information theory

Marlene Kretschmer (1,2, *), Fiona R. Spuler (2,1), Lluís Palma (3), Francisco Doblas Reyes (3, 4), Markus Donat (3,4), Llorenç Lledó (5a), Christopher D. Roberts (5b), Antje Weisheimer (5b,6), Theodore G. Shepherd (2,7)

(1) Leipzig Institute for Meteorology, Leipzig University, Germany
(2) Department of Meteorology, University of Reading, Reading, UK
(3) Barcelona Supercomputing Center (BSC), Barcelona, Spain
(4) Institució Catalana de Recerca i Estudis Avançats (ICREA), Barcelona, Spain
(5a) ECMWF, Bonn, Germany
(5b) ECMWF, Reading, UK
(6) Department of Physics, National Centre for Atmospheric Science (NCAS), University of Oxford, UK
(7) Jülich Supercomputing Centre, Forschungszentrum Jülich, Jülich, Germany

* corresponding author: marlene.kretschmer@uni-leipzig.de

This paper is a non-peer reviewed preprint submitted to EarthArXiv. The preprint was submitted to the Quarterly Journal of the Royal Meteorological Society (QJRMS) for consideration as a research article.

Abstract

Understanding the role of large-scale teleconnections in driving extreme weather is essential for improving the prediction and projection of climate extremes. Diagnosing the strength of teleconnection pathways, including their combined and modulated effects, is often based on composite or correlation analysis. However, such approaches become difficult to interpret in the presence of nonlinear relationships and when studying interactions across timescales. Here, we introduce (conditional) mutual information as a diagnostic tool to quantify teleconnection pathways in a systematic and unified framework. Embedded within a causal network describing the assumed relationships, this non-parametric measure of statistical dependence allows multivariate interactions to be summarized in a single metric. It can be used to compare the influence of different drivers across regions or to assess the temporal evolution of teleconnection strength for specific types of extreme events. The framework is illustrated by applying it to winter cold and wet extremes in Europe and North Africa, focusing on subseasonal drivers—the Madden–Julian Oscillation (MJO) and the stratospheric polar vortex (SPV)—and their modulation by seasonal drivers, namely El Niño Southern Oscillation (ENSO) and the Quasi-Biennial Oscillation (QBO). The results show that seasonal drivers influence both the occurrence of subseasonal drivers and their impact on surface extremes. These modulating effects persist across subseasonal timescales, suggesting periods of enhanced predictability. The proposed approach provides a diagnostic for identifying windows of forecast opportunity and offers a basis for evaluating the representation of teleconnections in climate models.

1. Introduction

European winter weather extremes, such as cold spells and heavy precipitation, represent major hazards with often severe societal and economic impacts. Cold extremes, for instance, have been associated with increased mortality (Charlton-Perez et al. 2021) and heightened risks of energy shortfalls during peak demand periods (Rouges et al. 2025). Similarly, wet extremes can lead to extensive winter flooding, resulting in widespread infrastructure damage, economic losses, and disruptions to communities (Chaqdid et al. 2023). Given these consequences, reliable forecasts for such extreme events are essential for effective decision-making and risk management across sectors including public health, energy supply, and disaster response.

However, the predictions of these extremes—particularly on subseasonal to seasonal (S2S) timescales—remain highly uncertain due to the inherently chaotic nature of the atmosphere (Vitart and Robertson 2018). While short-range weather forecasts can provide skillful guidance up to about two weeks, predictive skill typically declines sharply beyond this range, often dropping below that of a simple climatological baseline. Seasonal outlooks that aim to anticipate the overall severity or character of an upcoming winter season are likewise characterized by large uncertainties (Weisheimer et al. 2019). In contrast to traditional weather forecasting, S2S prediction research is further challenged by the limited availability of verification data, making it crucial to understand why a model exhibits or lacks predictive skill. Consequently, elucidating the physical drivers and mechanisms underlying extreme weather variability is a central step toward improving forecast reliability.

Large-scale atmospheric teleconnections are known to modulate regional weather and can create favorable conditions for the occurrence of extremes. These teleconnections can occasionally lead to periods when forecast skill is enhanced, a concept described as a “window of opportunity” (Mariotti et al. 2020). Recognizing and quantifying these windows is valuable for early warning systems and enhances the interpretability of model predictions. Accordingly, identifying the links between teleconnection patterns and European winter extremes is an active area of research (Spuler et al. 2024; Bommer et al. 2025).

For Europe and North Africa, the stratospheric polar vortex (SPV) and the Madden–Julian Oscillation (MJO) are among the most influential subseasonal drivers of extreme winter weather (Cassou 2008; Baldwin and Dunkerton 2001). Weak states of the SPV are typically followed by a southward shift of the North Atlantic jet stream, leading to below-average temperatures and more frequent cold extremes over Northern and Central Europe (Kretschmer et al. 2018), as well as enhanced precipitation in the Mediterranean region, particularly over the Iberian Peninsula (Spuler et al. 2025; Ayarzagüena et al. 2018). Conversely, strong vortex states tend to be associated with opposite-signed surface impacts. The MJO, in turn, modulates North Atlantic circulation by influencing Rossby wave propagation, with specific MJO phases linked to anomalous temperature and precipitation patterns across Europe (Lee et al. 2019). Although extreme SPV states such as sudden stratospheric warmings (SSWs) and active MJO phases persist only for a few days, their surface impacts can remain predictable for up to several weeks due to the oscillatory and quasi-periodic nature of

these systems (Hitchcock and Simpson, 2014). This property makes both the SPV and MJO key sources of predictability—and thus important windows of opportunity—for S2S winter weather forecasting.

While the roles of the SPV and MJO in shaping European weather and extremes are well documented, their variability and surface impacts are modulated by seasonally dependent background conditions such as the Quasi-Biennial Oscillation (QBO) and El Niño–Southern Oscillation (ENSO) (Lee et al. 2019; Ma et al. 2023; Elsbury et al. 2024). For example, winters characterized by an easterly QBO tend to exhibit a weaker SPV (Holton and Tan 1980), and also more active phases of the MJO (Son et al. 2017; Zhang and Zhang 2018). It has further been demonstrated that MJO and SPV teleconnections to Europe differ depending on the concurrent ENSO phase, implying that these large-scale modes not only favour certain MJO or SPV states but may also modulate their surface responses through additional, possibly nonlinear, processes (Lee et al. 2019; Kumar et al. 2022). However, such modulating effects and potential non-linearities are not yet fully quantified or well understood, underscoring the need for a more systematic assessment of state-dependent teleconnection behavior (Wang et al. 2025).

Understanding teleconnections and their role in driving extreme events, thus, remains difficult. In the context of S2S predictions, existing approaches to diagnosing windows of opportunity often rely on model-based skill assessments, which can conflate the physical teleconnection mechanisms with the validity and performance of the model (Albers and Newman 2019; Specq and Batté 2022). For instance, while most dynamical forecast systems are capable of representing the MJO itself, their simulated teleconnections to Europe are underestimated. Consequently, the predictive potential of the MJO as observed in reanalysis data is likely not fully exploited in operational forecasts (Specq and Batté 2022; Roberts et al. 2023). Evaluating how well a teleconnection signal is captured in models is further complicated by the fact that discrepancies between models and observations may arise from model biases, non-stationary relationships, or a combination of both.

Quantifying teleconnection signals is methodologically challenging because results are sensitive to the choice of statistical metrics and the representation of underlying variables. Correlation is commonly used to measure co-variability, but is suboptimal when common drivers or nonlinear interactions are present (Kretschmer et al. 2021). In studies focusing on extremes—often represented as binary, threshold-based events—computation of odds ratios or composites given different phases of remote drivers are often employed, thereby also allowing non-linear measures of association (Kumar et al. 2022). However, such approaches become cumbersome and data-intensive when multiple drivers or categorical states are considered (Jenney et al. 2019). For example, when analyzing MJO impacts across its nine canonical phases (eight active and one inactive), and further conditioning on three ENSO backgrounds (La Niña, El Niño, neutral), a total of 27 composites would be required, making rapid interpretation challenging.

Diagnosing teleconnection influences is further complicated given limited observational records and can result in under-sampled categories. Additionally,

methodological choices such as the representation of teleconnection driver (e.g., the ENSO index used, the metric and pressure level to define SPV states) or the partitioning of data (e.g., QBO defined by zonal-mean wind direction or via empirical orthogonal functions) are often context-dependent and can substantially influence the inferred relationships.

In summary, quantifying teleconnection signals and their relevance for extreme events is inherently a multivariate problem, as several interacting climate drivers can jointly influence regional weather on different timescales. These interactions can be nonlinear and state-dependent, making it difficult to separate individual effects. Moreover, since extremes and teleconnection drivers are commonly represented as binary or stratified data, such analyses typically require categorical data approaches rather than linear correlations. Together, this complicates the identification of windows of opportunity and the comparison of results across models and observations.

To better isolate the causal effects of teleconnections on regional weather, recent studies have adopted causal inference frameworks that incorporate physical knowledge into statistical analysis. Kretschmer et al. (2021) argued that, by starting from physically motivated causal networks, it is possible to control for confounding influences and isolate specific cause–effect relationships in teleconnections. Such approaches, rooted in the explicit formulation of physical assumptions as directed acyclic graphs (Pearl 2009), have since been applied more broadly in the study of teleconnections (Hamed et al. 2023; Carvalho-Oliveira et al. 2024; Di Capua et al. 2024; Kretschmer et al. 2020). However, most existing applications have relied on linear methods only (Cosford et al. 2025; Mindlin et al. 2025). To account for slowly varying background states, Shen et al. (2025) proposed a pre-conditioning of the data before estimating regression coefficients, with similar strategies also adopted by Di Capua et al. (2019) in the context of causal discovery. Thus, while causal inference has proven useful for quantifying teleconnection pathways, its use remains largely confined to linear relationships with a few examples of expressing causal dependencies among categorical data using conditional probability tables (Barnes et al. 2019; Kretschmer et al. 2021; Saggioro et al. 2024)1).

A different line of research has drawn on information theory, to detect and quantify nonlinear causal interactions. Originating from the seminal work of Shannon (1948), information theory provides a general, non-parametric framework to quantify statistical dependence. Within this framework, *mutual information* (MI) measures the total shared information between two variables, which is formulated as the reduction in uncertainty of one variable given knowledge of another. Runge et al. (2012) showed that *conditional mutual information*, that is, the extension to the multivariate case, serves as a robust measure of causal effect strength in time-series that can be applied to both categorical and continuous data (Kraskov et al. 2004). This work was built upon Ebert-Uphoff (2007) who applied it to quantify link strength in Bayesian networks, following earlier introductions in the context of probabilistic reasoning (Lauritzen and Spiegelhalter 1988; Pearl 1988).

More recent studies have employed information-theoretic tools in the context of S2S predictions. For example, Saggioro et al. (2024) used mutual information-based

methods to quantify the predictability of the southern hemisphere jet in response to large-scale winter/spring drivers based on a causal network. Furthermore, Spuler et al. (2025) applied mutual information and entropy to assess the predictability of North Atlantic weather regimes given knowledge of states such as the SPV and MJO. The application of entropy-based metrics in this context follows a long-standing tradition in meteorology and climate science of using information theory to assess predictability (e.g. DelSole and Tippett 2007; DelSole 2004; Leung and North 1990). Collectively, these studies demonstrate that information theory is well established in meteorology and climate science as a framework for quantifying predictability, while it also has a proven role in the study of causal effect estimation, including for teleconnections.

Motivated by the challenges of S2S predictions, this study combines information theory with causal reasoning to quantify how much information teleconnections provide about extreme winter weather in Europe and the Mediterranean under varying background states. Specifically, we compute the conditional mutual information between key subseasonal drivers—the SPV and the MJO—and the occurrence of cold and wet extremes, while conditioning on the seasonal driver states of the QBO and ENSO. This allows us to assess how the informational influence of the SPV and MJO on surface extremes is modulated by slower-varying climate modes.

2. Data

We use daily ERA5 reanalysis data for the period 1950–2020. The selected indices follow a causal network framework, with the considered pathways illustrated in the schematic network shown in Fig. 1a including both subseasonal (SPV, MJO) and seasonal (QBO, ENSO) drivers.

We consider two types of extreme events: *cold extremes*, defined as periods when the 7-day averaged linearly detrended surface air temperature falls below the 10th percentile, and *wet extremes*, defined as periods when the 7-day averaged detrended total precipitation exceeds the 90th percentile. The detrending and the calculation of percentile thresholds are performed over the full winter time series at each grid point independently. Extremes are identified at each grid point, with the first day of the 7-day averaging window used as the event label. Our analysis is restricted to winter events (December–March) and leap days have been excluded. Note that, by construction, an extreme event starting on 31 March includes data from the first six days of April.

To assess the state of the SPV preceding the extreme events, we construct a categorical SPV time-series based on daily 100 hPa zonal-mean zonal winds averaged over 60-75°N. We use 100 hPa instead of the commonly used 10 hPa, as this lower stratospheric level was shown to better capture the downward influence of the SPV (Karpechko et al. 2017) and is also more closely linked to polar night jet events (see e.g. supplementary information in Kretschmer et al. 2018). From the daily SPV data, we then form the 7-days running mean and remove the smoothed daily climatology to obtain anomalies. To make sure that for a given winter day the driver state only contains information preceding in time, the data is shifted back by 6 days compared to

the extreme event data. For example, the SPV value on March 31 consists of the March 25-31 average. This time-shift between driver and extreme event is also schematically indicated in Figure 1b. To obtain categorical data, we compute the terciles of the SPV timeseries, resulting in low, neutral and strong SPV days.

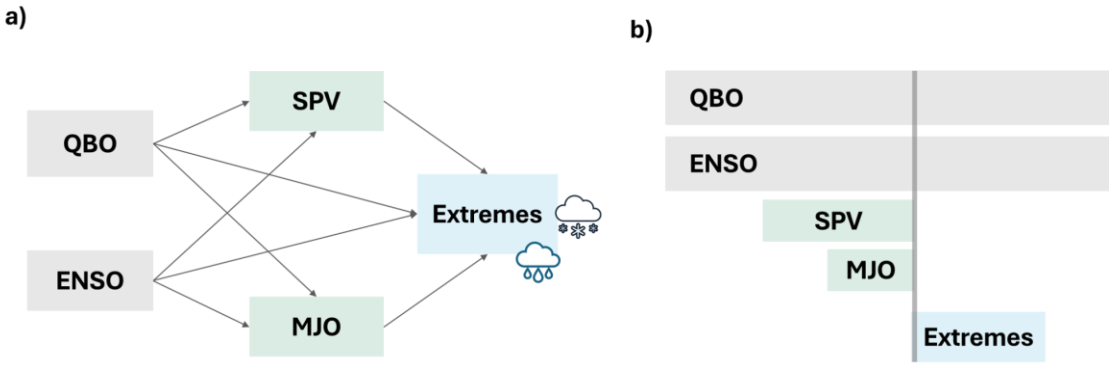

Figure 1: a) Causal network showing the considered seasonal (QBO and ENSO) and subseasonal (SPV and MJO) drivers of extreme events, with the arrows indicating assumed causal pathways. b) Schematic overview of included time-shifts and scale of the data (see text for details). The vertical line marks a winter day for which the states of the extremes and drivers are evaluated.

To assess the MJO state, we use the daily real-time multivariate (RMM) index (Wheeler and Hendon 2004). The MJO is considered active when the amplitude exceeds 1 standard deviation, with the phase of the MJO ranging from 1 to 8 and reflecting different locations of increased convection in the tropical Pacific.

For the seasonal drivers, we diagnose their phase based on average winter conditions. ENSO is defined using daily sea-surface temperatures in the Niño 3.4 region (5°S–5°N, 170°W–120°W), averaged over December–February (DJF). A winter is classified as El Niño when the DJF mean exceeds +0.4 K, as La Niña when it falls below −0.4 K, and as neutral otherwise.

The QBO phase is determined from zonal-mean zonal wind at 50 hPa averaged over the Tropics (10°S–10°N). Following Yamazaki et al. (2020), winters with positive DJF-mean winds are classified as westerly QBO (WQBO), those with negative zonal winds as easterly QBO (EQBO). This approach, while not explicitly capturing the vertical structure or descent of the shear zones, is appropriate here given the relatively small sample size.

To further showcase our framework for assessing teleconnection information on S2S timescales, we additionally consider two regional extreme events. We focus on wet extremes in Morocco and cold extremes in the UK, two hazards linked to high impacts (Charlton-Perez et al. 2021; Mastere et al. 2025) and further known to be affected by SPV and MJO variability (Spuler et al. 2025; Monnin et al. 2022). These regional indices are constructed by first computing area-averaged temperature over the UK (6°W-1.5°E, 50-59°N) and precipitation over Morocco (11-0°W, 30-36°N). We then proceed as described above to identify extreme events. To evaluate the predictive

information content of the drivers at different lead times, we analyse their relationship with extreme events occurring in subsequent weeks, considering lead times from 1 to 6 weeks.

In total, this yields 8501 winter days, with 10% of these considered as extreme events. The SPV and ENSO states are each divided into three categories, while the QBO is treated as a binary variable. The corresponding sample sizes for the seasonal-subseasonal drivers combinations are provided in Table S1 and S2 in the Supplementary Information.

3. Methods

We apply measures from information theory, namely mutual information and conditional mutual information, to quantify causal effects of teleconnection drivers on extreme events. As stated in the introduction, this choice of statistical measure follows earlier work (Ebert-Uphoff 2007; Pearl 1988; Lauritzen and Spiegelhalter 1988; Runge et al. 2012). While the focus in Runge et al. (2012) was on causal discovery (that is, on identifying causal links from data and then quantifying their strength), we here constrain the problem to only quantifying the link strength and assume a causal structure of the considered variables (Saggioro et al. 2024).

Our assumptions are expressed in the form of a causal network (see Fig. 1a). More precisely, we assume that both SPV and MJO affect the frequency of cold and wet extreme events across Europe and North Africa. We further postulate that the seasonal drivers ENSO and QBO are independent and can both affect the subseasonal drivers, while also modulating extreme event occurrence directly, represented as a common driver of the subseasonal drivers and extremes. We here ignore potential causal dependencies between the two subseasonal drivers (Barnes et al. 2019).

We aim to quantify how strongly teleconnection drivers (MJO, SPV, ENSO, QBO) are associated with the occurrence of cold and wet extremes. Because the climate system is inherently stochastic, the occurrence of an extreme event remains uncertain even when the state of these drivers is known. We therefore require a measure of association—analogous to correlation—that quantifies how knowledge of a driver reduces this uncertainty.

In information theory, the uncertainty of the outcome of a random process Y (here a categorical variable) is expressed by its ***entropy*** H, and is defined as $H(Y) = -\Sigma_i p_i \cdot ln(p_i)$, where p_i denotes the probability of the ith outcome of Y. For example, for Y representing a coin flip with probability $p = 0.5$ for each side, the entropy of Y is given by:

$$H(\text{“}fair\ coin\text{”}) = -(0.5 \cdot ln(0.5) + 0.5 \cdot ln(0.5)) = -ln(0.5) = 0.693.$$

In contrast, the entropy of a loaded coin flip, with probability $p = 0.9$ for landing on one side (thus, serving as the coin analogue of our percentile-based extreme event definition), is

$$H(\text{“}loaded\ coin\text{”}) = -(0.9 \cdot ln(0.9) + 0.1 \cdot ln(0.1)) = 0.325.$$

In other words, the outcome of the fair coin is more uncertain than that of the loaded one.

The strength of association of two (categorical) variables X and Y is then measured by their ***mutual information***, $I(X;\ Y)$ (see also Fig. 2). This quantifies the reduction in uncertainty of Y, given knowledge of X:

$$I(X;\ Y) = \ H(Y)\ -\ H(Y|X)$$

It is zero if and only if X and Y are independent, and positive otherwise. The larger the mutual information, the more the uncertainty about Y is reduced by knowing X, and the more information X provides about Y (see also Fig. 2 for an example for a binary variable X). Mutual information is a nonparametric and symmetric measure of association, meaning that $I(X;\ Y)$ = $I(Y;\ X)$, analogous to correlation but capable of capturing nonlinear relationships.

To illustrate this concept, consider the mutual information of a driver X with two equally likely states and a skewed binary variable Y with probabilities $p_0\ = 0.9$ and $p_1\ = 0.1$ (grey bars in Fig. 2). If the conditional distributions $p(Y|X)$ are similar to the marginal distribution, for example $p(Y = 0 \mid X = 0) = 0.88$ and $p(Y = 0 \mid X = 1) = 0.91$ (blue bars in Fig. 2), this yields conditional entropies similar to $H(Y) = 0.325$, here $H(Y \mid X = 0) \approx 0.346$ and $H(Y \mid X = 1) \approx 0.303$. The conditional entropy $H(Y \mid X)$ then is their weighted mean (weighted by probability of outcome X, i.e. $p_i\ = 0.5$), leading to a mutual information of X and Y close to zero. In other words, observing X provides little additional information about Y. In contrast, if the conditional distributions differ more strongly from the marginal (e.g., $p(Y = 0 \mid X = 0) = 0.81$ and $p(Y = 0 \mid X = 1) = 0.99$ (purple bars in Fig. 2), this leads to markedly different conditional entropies ($H(Y \mid X = 0) \approx 0.486$, $H(Y \mid X = 1) \approx 0.056$) and a substantially smaller weighted conditional entropy $H(Y \mid X)$. This larger reduction in uncertainty corresponds to a larger mutual information.

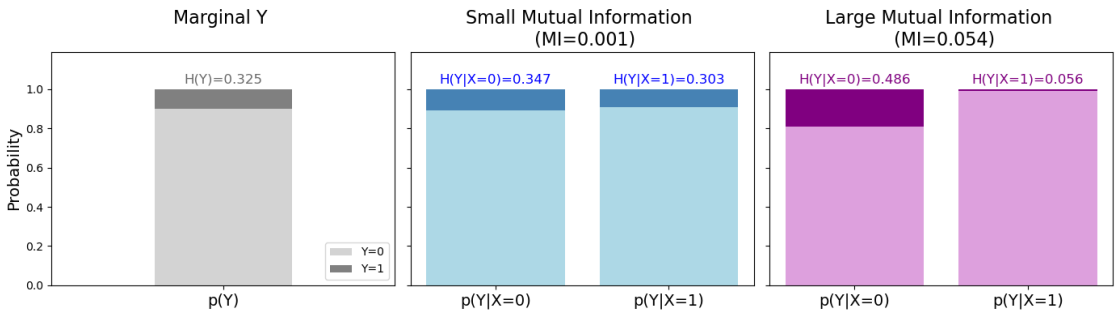

Figure 2: Illustration of mutual information for a skewed binary variable Y and a binary driver X with two equally likely states. The left panel shows the marginal distribution of Y as a stacked bar (gray) with probabilities [0.9,0.1]. The middle and right panels show the conditional distributions p(Y/X=0) and p(Y/X=1) as stacked bars for the small (blue) and large (purple) mutual information examples. The conditional entropies H(Y/X=x) are annotated above each bar. See text for more details.

Conditional mutual information $I(X; Y|Z)$ then measures the reduction in the uncertainty of Y given Z when X is also known. It thus quantifies the amount of additional information that X provides about Y beyond what is already known from Z:

$$I(X;Y \mid Z) = H(Y \mid Z) - H(Y \mid X,Z).$$

The conditional mutual information is zero if and only if X and Y are independent given Z.

These properties illustrate why information theory serves as an intuitive non-parametric framework for causal effect estimation: If X is a causal driver of Y but its effect is fully mediated via Z, then we want their statistical association to be zero, which is the case for their conditional mutual information. Similarly, the conditional mutual information is zero if Z is a common driver of X and Y. In both cases, the (unconditional) mutual information between X and Y would nevertheless be non-zero. This is fully analogous to using well-established correlation for the linear case, where, for instance, a common driver Z leads to a non-zero correlation of two variables, which drops to zero when computing the partial correlation conditional on Z (see also Kretschmer et al 2021 Figure 3, for real-world teleconnection examples).

Finally, the difference between the mutual information $I(X; Y)$ and the conditional mutual information $I(X; Y|Z)$ (also referred to as interaction information) quantifies how much information is shared jointly, including redundancy and synergy effects. If the mutual information exceeds the conditional mutual information, this indicates that X and Z provide overlapping information about Y. This is the case when Z is a mediator between X and Y, or when Z is a common driver of both variables. In contrast, when the conditional mutual information I(X;Y|Z) exceeds the mutual information I(X;Y), then conditioning on Z reveals additional dependence between X and Y, that is not apparent from their marginal association I(X;Y) alone. This situation arises when X and Z jointly influence Y. In the linear analogue, this corresponds to obtaining more precise estimates of causal effects when jointly regressing on X and Z rather than considering each predictor separately (see, e.g., Cinelli et al. 2020). This phenomenon is conceptually related to Simpson's paradox, where aggregating over a third variable can obscure or even reverse statistical relationships (Pearl 2013).

In the present work, we use (conditional) mutual information to quantify the information that a teleconnection driver provides about a given type of extreme event, including modulation arising from synergistic effects. Because mutual information values are relative and lack an intrinsic scale, in some parts we normalize them by the climatological entropy of the corresponding extreme threshold, which is 0.325 for both the 10th percentile (cold extremes) and the 90th percentile (wet extremes). This normalization expresses mutual information as the percentage reduction in total uncertainty.

Furthermore, given the low number of samples in each of the categories, we apply a block bootstrapping approach to assess the uncertainty of the estimates throughout

the different analyses. We hereby sample entire seasons from the data rather than individual datapoints, to account for the autocorrelation of the data, and assess the distribution of estimates on 100 different subsamples of seasons. This provides an assessment of potential intermittency and non-stationarity of the effects identified.

4. Results and Discussion

4.1. Diagnosing teleconnection strengths with mutual information

To illustrate the use of mutual information as a teleconnection diagnostic, we begin on the left side of the causal network (Fig. 1a) and quantify the information that seasonal drivers (QBO, ENSO) provide about the subseasonal drivers (SPV, MJO). Specifically, we compute the mutual information $I(X;Y)$ between each seasonal driver X and each subseasonal driver Y. Mutual information is formally symmetric, but given the temporal structure of the system—where ENSO and QBO states are defined once per winter, while MJO and SPV vary on subseasonal timescales—we interpret this quantity as the information that knowledge of the seasonal drivers provides about the subseasonal state.

The results are shown in Fig. 3 (gray bars) as box-and-whisker plots based on bootstrapped subsamples (see Methods). As an illustrative example, consider first the QBO-SPV pair (Fig. 3a), an established linkage that reflects the well-known Holton-Tan effect (Anstey et al. 2022). Albeit having a large spread, we find a comparatively strong mutual information signal (mean value of 0.019). This quantifies the association between QBO and SPV, summarizing underlying conditional probability distributions (see also Table 1 in SI): during easterly QBO, the distribution of SPV states shifts away from climatological frequencies toward more weak (40%) and fewer strong (25%) vortex states, while during westerly QBO the distribution shifts opposite accordingly (27% weak, 32% neutral, 41% strong). In other words, knowledge of the QBO provides information about the likely SPV state, and mutual information quantifies this shift as a reduction in uncertainty. Although the mean absolute value of $I(QBO;SPV)$ is modest—corresponding to a reduction of approximately 2% of the SPV entropy—this magnitude is expected, as the winter QBO index represents only one of several drivers of subseasonal SPV variability.

Having established this interpretation, we move to the other seasonal–subseasonal driver pairs. In contrast to the QBO–SPV association, the mean and spread of the mutual information between ENSO and the SPV (Fig. 3a) is substantially smaller, reflecting a weaker coupling. For the MJO, we find that QBO and ENSO provide comparable levels of information (Fig. 3b), suggesting a similar influence of both seasonal drivers on subseasonal tropical variability.

We next repeat these computations, but now condition on the state of the other seasonal driver; that is, we compute the conditional mutual information $I(X;Y|Z=z)$. This follows the rationale of the causal network, in which both QBO and ENSO are assumed to contribute to modulating SPV and MJO variability. Including both seasonal drivers

in the conditioning set therefore provides a more precise estimate of the causal effect by controlling for shared influences (Cinelli et al. 2020). From a mechanistic perspective, this can be interpreted as quantifying the influence of one driver under a fixed background state of the other, thereby revealing how their effects combine, interfere, or depend on each other across different climate states (Elsbury et al. 2026).

When computing these conditional mutual information values we find elevated values for most seasonal-to-subseasonal linkages (coloured box plots in Fig. 3). For example, the information of ENSO about the SPV when conditioning on an easterly QBO state (I(ENSO;SPV|QBOE) roughly triples, and a similar increase occurs when conditioning on QBOW (Fig. 3a). This result is consistent with recent findings using linear regression and toy-model experiments (Shen et al. 2026, under review), which suggest that the ENSO–SPV linkage should not be studied in isolation

Interestingly, the high mutual information between QBO and SPV conditional on ENSO is primarily driven by large values during La Niña winters (Fig. 3a). This is in agreement with Kumar et al. (2022) who reported an enhancement of the QBO on SPV effect during La Niña, which was absent during El Niño. In contrast, the ENSO–SPV linkage remains similarly strong across both QBO phases. For the MJO, El Niño conditions are associated with lower mutual information between QBO and MJO than La Niña or neutral conditions, while the easterly QBO phase leads to less information from ENSO compared to the westerly QBO phase (Fig. 3b). This is consistent with previous findings that the easterly QBO is associated with more active MJO phases (Zhang and Zhang 2018), but potentially in conflict with recent model comparisons reporting a lacking QBO-MJO coupling when controlling for ENSO (Elsbury et al. 2026). Overall, the spread of conditional effects on the MJO is smaller than that for the SPV, indicating that the latter exhibits a stronger dependence on the seasonally varying background state.

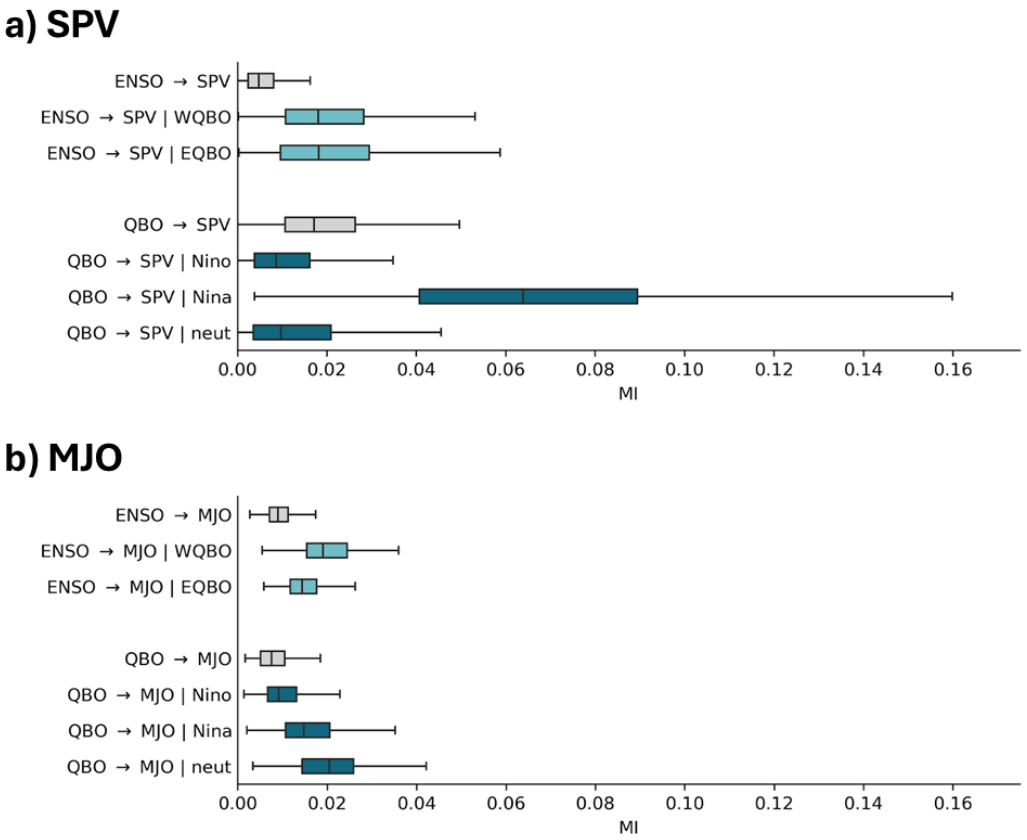

Figure 3: Mutual information (in grey) and conditional mutual information (in blue and turquoise) of the seasonal drivers and subseasonal drivers. a) for the SPV, and b) for the MJO. The box and whiskers plots show the uncertainty based on a bootstrap approach (see Methods). The specific condition used to compute mutual information is indicated on the y-axis.

4.2. Teleconnection drivers of cold and wet extremes

Moving along in the causal network (Fig. 1a), we next assess the information content of the considered subseasonal (SPV, MJO) and seasonal (QBO, ENSO) drivers for the occurrence of cold and wet extremes in the following week, by computing the (unconditional) mutual information, that is, I(X=driver;Y=extreme). The results are shown in Figure 4. To aid interpretation, we here express mutual information as a percentage of the climatological uncertainty of cold and wet extremes (see Methods).

For the SPV, the mutual information with cold extremes shows expected regions of influence. Elevated values are found across Northern Europe and parts of Northern Africa, consistent with known surface impacts of stratospheric variability on temperature extremes (e.g., Domeisen and Butler 2020; Monnin et al. 2022). In contrast, mutual information is lower over Southern Europe, where the SPV exerts a weaker influence on near-surface temperatures. For wet extremes, the SPV shows enhanced information in the Mediterranean region, as well as over Scotland and Norway (Fig. 1b). These patterns are consistent with the well-documented impacts of the SPV strength on the position and intensity of the North Atlantic jet and storm tracks,

which modulate the transport of moisture toward Europe (Afargan-Gerstman et al. 2024).

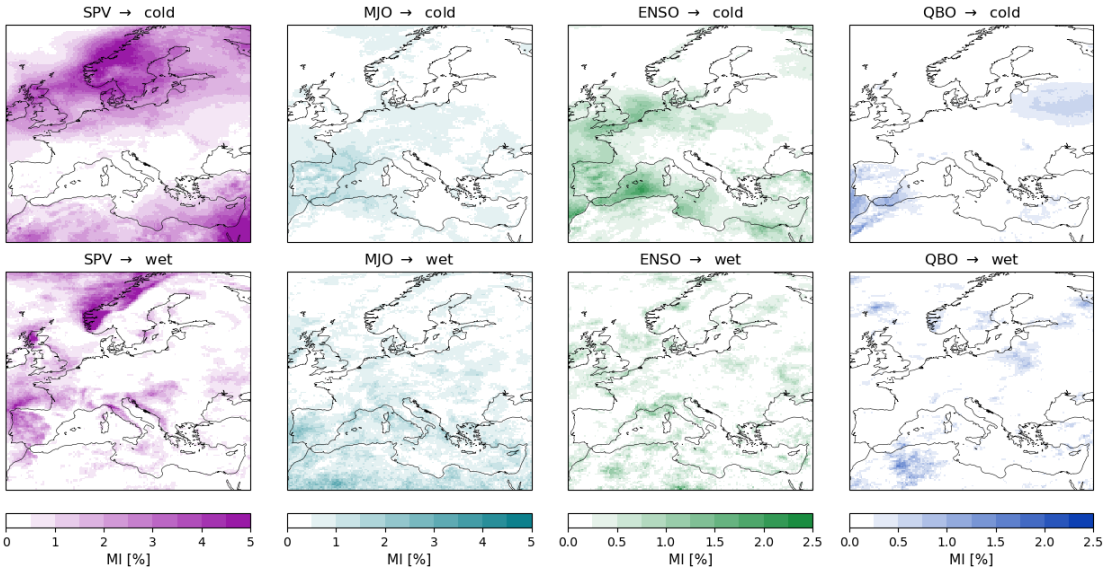

Figure 4: Mutual information (expressed as a percentage of the climatological entropy of the extreme event) of different drivers (SPV, MJO, ENSO, QBO) and extreme events (cold and wet). Note the smaller colourbar range for ENSO and QBO.

Note that while the mutual information is rather small, the drivers are informative in specific states. For example, in Northern Europe, knowledge of the SPV state, on average, only leads to a reduction of about 5% of the climatological uncertainty of a cold extreme (Fig. 4a), but the probability of an extreme given a weak polar vortex state approximately doubles (see also Fig. S1), as is also well known (Monnin et al. 2022; Domeisen and Butler 2020). The mutual information can be sensitive to the threshold used to compute extremes. However, here the aim is not to maximise the mutual information by using different percentiles to define extreme events, or by choosing different thresholds to stratify the drivers (e.g. using the lower quartile instead of the lower tercile to categorize weak SPV states), but rather to introduce it as a diagnostic metric and compare the modulation of drivers by seasonal driver states (as shown later), thus justifying our choice of simple and widely used driver and extreme event categories.

For the MJO, we find generally lower mutual information values compared to the SPV, but the spatial distribution is more homogeneous across Europe and North Africa. This reflects the diversity of teleconnection pathways associated with different MJO phases. For example, MJO phase 1 is associated with an increased likelihood of cold extremes in the southern Mediterranean, while phase 7 tends to enhance cold risk in Central Europe (see Fig. S2). Because mutual information summarizes the dependence across all nine MJO states, it naturally dilutes the signal of individual phases that may dominate in specific regions. In contrast, weak, neutral, and strong SPV states each affect the same regions across the continent with odds ratios similarly high as for individual MJO phases. As a result, aggregating over SPV states does not blur away the signal. Thus, it should be noted that the overall lower mutual information associated

with the MJO must be interpreted in light of the chosen representation of the MJO state. Alternative indices to the real-time multivariate MJO (RMM) index used here (Wheeler and Hendon 2004) may better capture the physically relevant component of MJO variability for European teleconnections. As noted before, sensitivity to such representational choices is not explored in this study.

Turning to the seasonal drivers, both QBO and ENSO exhibit lower mutual information values compared to the subseasonal drivers (note the different colour scales in Fig. 4), as expected given their more indirect and slowly varying influence. For the QBO, enhanced signals emerge over southwestern and northeastern Europe, whereas ENSO exhibits stronger associations along a northwest–southeast axis. These spatial patterns are broadly consistent with the known modulation of North Atlantic and Mediterranean variability by these seasonal modes (Brönnimann 2007; Anstey et al. 2022).

Overall, these mutual information maps condense the insights typically obtained from multiple conditional probability or composite analyses for a given extreme type into a single intuitive diagnostic. For comparison, a traditional conditional-probability analysis would require separate panels for each driver state (17 per extreme: 3 SPV + 9 MJO + 3 ENSO + 2 QBO). The mutual information approach instead summarizes this information in a single panel per driver–extreme pair (see Figs. S1 and S2 for the individual conditional probability plots). This compact assessment efficiently summarizes the association between teleconnection states and extreme-event occurrence and provides a useful first step toward identifying regions where teleconnections offer predictive information.

4.3. Driver dependencies and modulating effects

We next assess how seasonal driver states modulate the impact of subseasonal drivers on extreme events. Specifically, we measure how the information a subseasonal driver (SPV, MJO) provides about extremes changes when conditioned on a seasonal driver (ENSO, QBO). Unlike the previous analysis, where both seasonal drivers influenced subseasonal drivers directly (see Fig. 1a), here their effect on extremes is at least partly mediated through the subseasonal drivers. For example, the predictive value of the QBO for cold extremes might arise primarily from its modulation of SPV and MJO states (Zhang and Zhang 2018; Anstey et al. 2022). For the ENSO, both direct and indirect pathways have been reported (Domeisen et al. 2019). One question here is whether knowledge of the seasonal driver adds information beyond the subseasonal driver, as represented by the direct seasonal-to-extreme links in our causal network (Fig. 1a), consistent with reported state-dependent teleconnection effects (Kumar et al. 2022; Wang et al. 2025).

To quantify these modulation effects, we compute the conditional mutual information $I(X;Y|Z=z)$ between each subseasonal driver X and extreme events Y, given the seasonal driver Z, and subtract the unconditional mutual information $I(X;Y)$ calculated over all winter days (as shown in Fig. 4). The difference reflects the synergistic effect

of the considered drivers and is again expressed as a percentage of the climatological uncertainty of an extreme to facilitate interpretation. The resulting difference fields are shown in Figure 5, highlighting regions where conditioning on seasonal drivers provides additional information beyond that contained in the subseasonal driver alone. Values close to zero therefore suggest weak or negligible modulation of the subseasonal effect by the seasonal background state.

For SPV–cold extreme linkages (Fig. 5a), conditioning on either the QBO or ENSO moderately enhances the information content in some regions, for example over the Baltic region. However, differences relative to the unconditional case remain small, suggesting generally limited modulation by seasonal drivers. The most striking exception is found for SPV influences on cold extremes in North Africa and Scandinavia during El Niño conditions, where the added information reaches up to 8% of the total climatological uncertainty. Over Scandinavia, this corresponds to nearly three times the information content of the unconditional mutual information (note the different colour-bar range used in Fig. 4). In contrast, the MJO exhibits different patterns in information gain for cold extremes when seasonal drivers are considered (Fig. 5b), with largest values for ENSO conditioning. During La Niña phases, enhanced information is found over Iberia, whereas during El Niño phases, increased information emerges over the UK, France, and the western Mediterranean. The added values, which are on the order of 5% of the total uncertainty, exceed the unconditional MJO-related mutual information shown in Fig. 4.

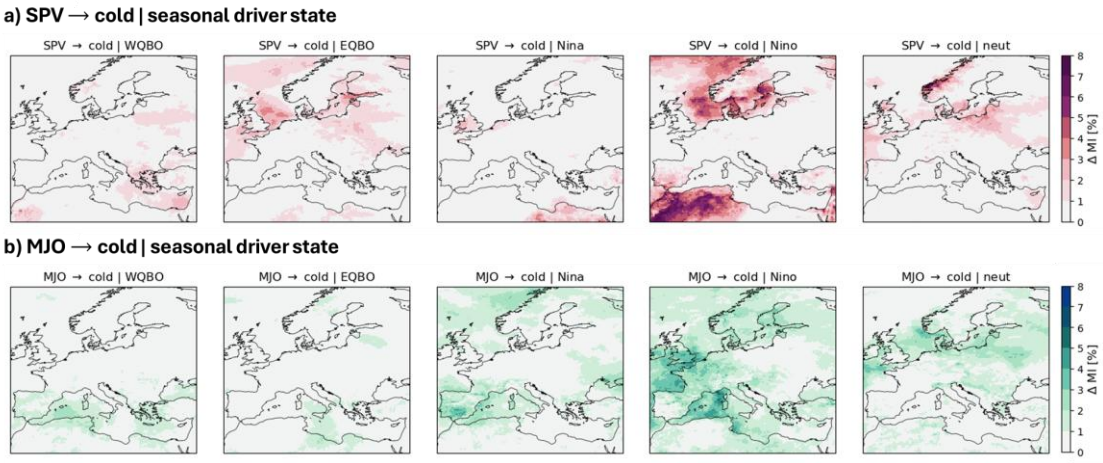

Figure 5: Seasonal modulation of subseasonal driver impacts on extreme events. Additional reduction in uncertainty of cold and wet extremes due to conditioning on seasonal driver states (WQBO, EQBO, La Niña, El Niño, ENSO-neutral), calculated as the difference between conditional mutual information and unconditional mutual information I(X, cold/Z=z) - I(X,cold) for a) SPV, and b) MJO. Note the larger colourbar range compared to Fig. 3.

For the SPV, conditioning on a seasonal driver state adds very little information for wet extremes (Fig. 6a), indicating that most of the seasonal influence is mediated through SPV, with some regional enhancements, for example during ENSO-neutral winters.

For the MJO, the magnitude of additional information for wet extremes is similar to that for cold extremes, although spatial patterns are more fragmented (Fig. 6b).

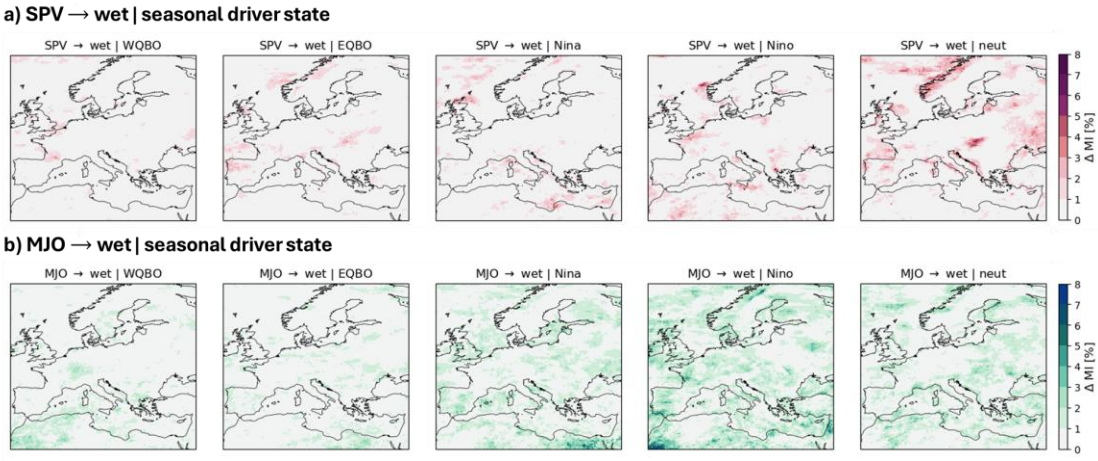

Figure 6: Same as Fig. 5 but for wet extremes.

Overall, while the unconditional mutual information between the SPV and extremes is larger than that between the MJO and extremes (Fig. 4), the *conditional* mutual information for the SPV appears mostly smaller (Fig. 5,6). This indicates that the effect of the SPV is less strongly modulated by the seasonal drivers compared to the MJO, which provides more distinct information on extremes when the seasonal drivers are included as conditioning variables.

In summary, these results demonstrate that ENSO and QBO modulate the SPV– and MJO–extreme weather relationships, supporting the hypothesis that slowly varying drivers shape the effectiveness and predictability of subseasonal teleconnections over Europe and the Mediterranean. More generally, such conditional analysis serves as a diagnostic framework to identify periods of enhanced information transfer, thereby highlighting *windows of opportunity* when and where predictive skill for extreme events may be increased, as we further explore in the following.

4.4. Regional analysis on subseasonal-to-seasonal (S2S) timescales

Thus far, our analysis has focused on extreme events occurring in the following week and conditioned on individual seasonal and subseasonal drivers. However, longer-lived influences are particularly relevant, especially given the limited skill of operational forecast models at S2S forecast times. We therefore extend the analysis to quantify the information content of large-scale drivers on extremes up to six weeks ahead.

For clarity, we focus on the influence of the SPV and MJO on cold extremes over the UK. This choice is broadly guided by earlier results (Figs. 4, 5) and motivated by examining both a well-established relationship (SPV–UK cold) and a less-studied one (MJO–UK cold), thereby providing new insights. The results are shown in Figure 7 as a heat map of mutual information between subseasonal drivers and regional extremes across lead times (x-axis) and conditioning levels (y-axis). To emphasize temporal evolution, we show mean values based on bootstrapped samples. To account for

uncertainty, we highlight cases where 75% of conditional mutual information values exceed the mean unconditional mutual information (indicated by the black contoured boxes).

For the SPV–UK cold relationship (Fig. 7a), we find non-zero mutual information across lead times (see also Fig. 4 for the first seven days), gradually decreasing with increasing lead time. Conditioning on seasonal states reveals periods of enhanced information at S2S timescales, particularly during the first three weeks under La Niña conditions and at longer leads during neutral ENSO. Conditioning on the easterly QBO phase also adds information, consistent with earlier results (Fig. 5a). When conditioning jointly on ENSO and QBO, elevated values emerge across most combinations and lead times, indicating synergistic effects. The highest mutual information occurs during easterly QBO and neutral ENSO conditions, substantially exceeding the unconditional case.

For the MJO–UK cold relationship (Fig. 7b), unconditional mutual information is lower than for the SPV, but conditioning on seasonal drivers leads to a consistent increase across lead times. Conditioning on ENSO generally provides more information than conditioning on the QBO alone, while the highest values arise when both are considered jointly. This pattern persists across lead times. The strongest MJO-related signal occurs during El Niño combined with westerly QBO, although similarly elevated values are found for easterly QBO and neutral ENSO. Overall, these results indicate that MJO influences on European weather for up to six weeks ahead are strongly modulated by the seasonal background state.

Repeating the analysis for Moroccan wet extremes yields qualitatively similar results (Fig. S3); Conditioning on both ENSO and QBO enhances information relative to the unconditional case, particularly for the MJO, where the signal remains strong across lead times. In contrast, SPV variability shares more intrinsic information with extremes, suggesting a more direct influence that is less dependent on seasonal modulation.

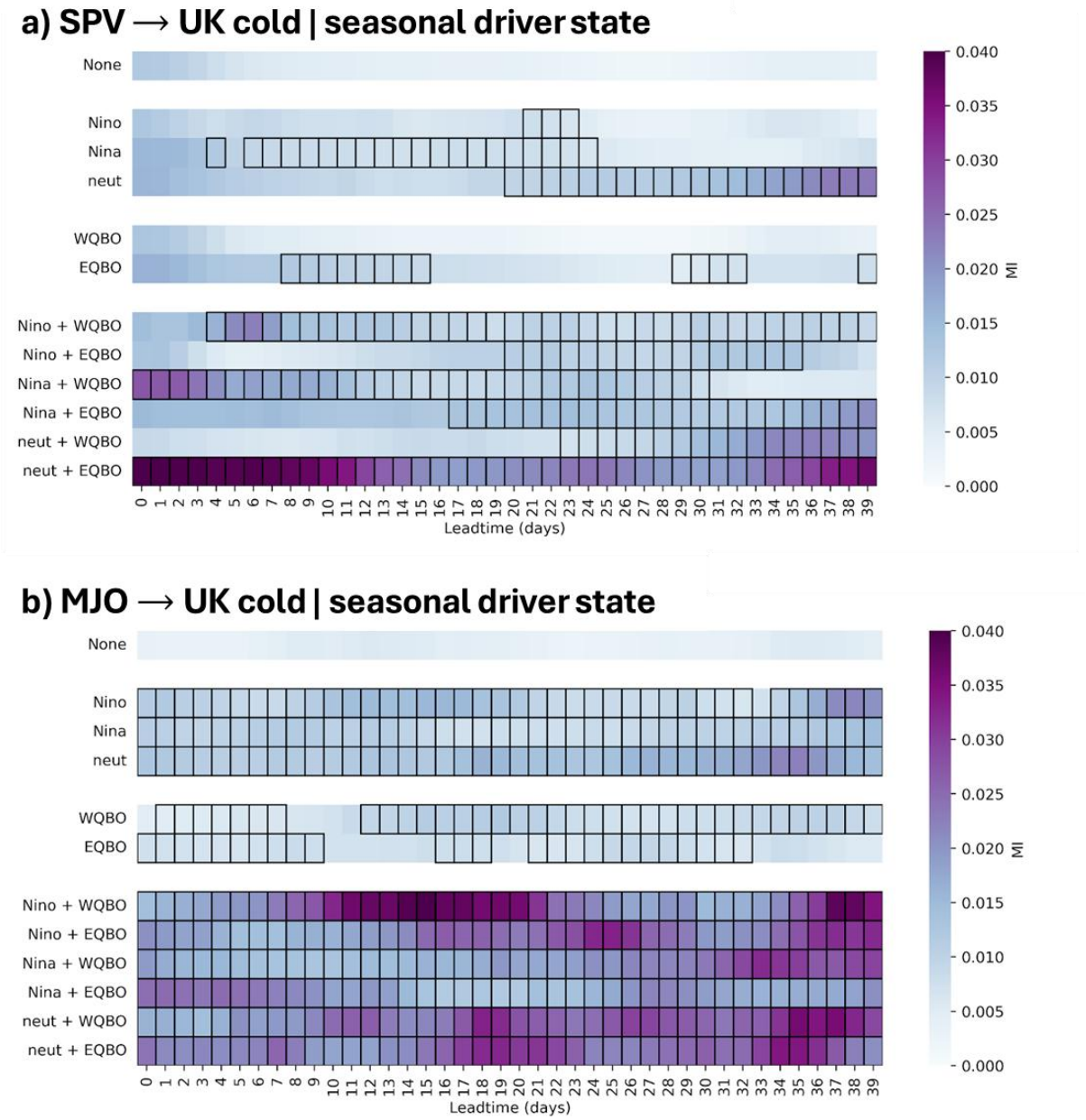

Figure 7: Lead-time-dependent information content of subseasonal drivers for regional extremes. Mutual information between (a) the SPV and UK cold extremes and (b) the MJO and UK cold extremes for lead times up to 39 days, shown for different levels of conditioning as indicated along the y-axis. Values represent bootstrapped mean estimates (see Methods). Contours indicate that 75% of bootstrapped conditional mutual information values exceed the mean unconditional mutual information (labeled "None" in the first row in each panel) for the respective lead-time.

From an S2S prediction perspective, periods of elevated mutual information highlight potential windows of enhanced forecast skill. ENSO and QBO states are typically

known or predictable at the start of the season, while subseasonal drivers can be monitored and forecast throughout winter. Identifying conditions under which seasonal drivers amplify subseasonal influences may therefore provide valuable guidance for S2S forecasting.

We further argue that such periods of elevated mutual information provide a starting point for more detailed dynamical investigation of associated large-scale circulation structures, hence the mediating processes. As an illustrative example, we composite mid-tropospheric circulation patterns, expressed as 500-hPa geopotential height anomalies, averaged over the ten days after strong and weak SPV phases and conditional on combinations of seasonal drivers, analogous to the analysis shown in Figures 5 and 6 and similar to what was done in Osman et al. (2022). These composites reveal distinct circulation responses across different background states.

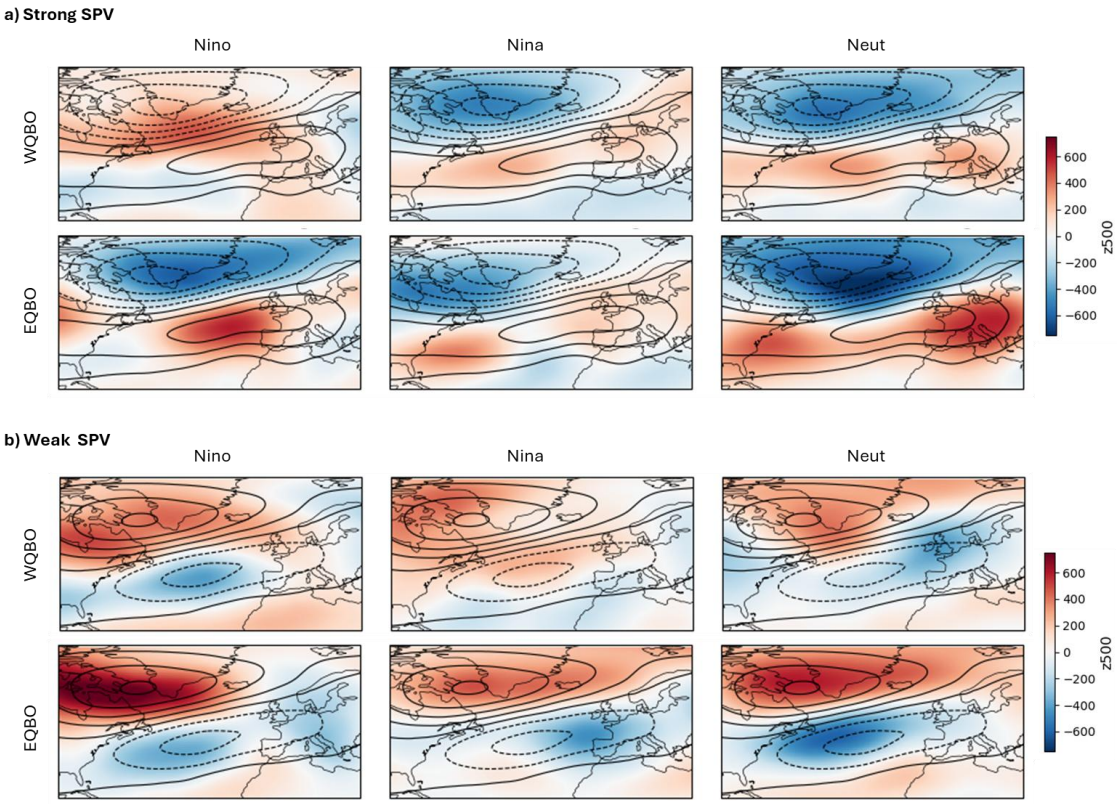

Figure 8: Composites of z500 anomalies (in metres) averaged over the 10 days after a) strong SPV states and b) weak SPV states, for different combinations of ENSO and QBO phases. The respective QBO and ENSO phases are indicated on the left and top of the panels. The contours indicate the average z500 anomalies during strong SPV (in a) and weak SPV (in b) without any seasonal conditioning. The sample sizes of each combination is shown in Table 1 in the SI.

For strong SPV states (Fig. 8a), the expected positive NAO-like pattern (see also contours) emerges across almost all seasonal driver phases and is particularly pronounced during neutral ENSO combined with an easterly QBO, consistent with the high SPV-cold mutual information for this phase combination (Fig. 7a). However, under El Niño conditions together with a westerly QBO, the circulation response exhibits a partly opposite-sign pattern, characterized by positive 500-hPa height anomalies south of Greenland and negative pressure anomalies over the subtropical North Atlantic. This pattern strongly projects onto the combined responses to El Niño and westerly QBO mean states (see Fig. S4), which appears sufficiently strong to suppress the canonical circulation response typically associated with strong SPV events. Note that this appears partly in contrast to the hypothesis that the prevailing synoptic-type weather regimes control the downward propagation of stratospheric anomalies (e.g., Domeisen et al. 2020). For weak SPV phases, the different configurations project onto a negative NAO-like pattern, consistent with expectations, albeit with variations in amplitude and spatial structure. In particular, a diluted signal given La Niña and westerly QBO is present, which explains the higher mutual information for this combination (Fig. 7a). Together, these analyses show that the enhanced mutual information of SPV and MJO for UK cold extremes given seasonal driver states (Fig. 7) can be explained through modulations of the North Atlantic atmospheric circulation, making the former a useful diagnostic to analyse pattern modifications. A comprehensive investigation of these pathways and modulation processes is beyond the scope of the present study but represents an important avenue for future research.

5. Summary and Conclusions

In this work, we apply (conditional) mutual information, a well-established non-parametric measure of statistical dependence, to quantify the influence of subseasonal and seasonal teleconnection drivers on cold and wet winter extremes across Europe and North Africa (Fig. 4). We show that the seasonal drivers El Niño–Southern Oscillation (ENSO) and Quasi-Biennial Oscillation (QBO) not only modulate the frequency of the subseasonal drivers Madden–Julian Oscillation (MJO) and Stratospheric Polar Vortex (SPV) (Fig. 3), but also alter their impact on surface weather extremes (Figs. 56). These modulating effects can persist across S2S timescales (Fig. 7), revealing periods of enhanced predictability of extremes arising from teleconnections. This, in turn, highlights potential windows of opportunity for prediction and provides a basis for investigating the underlying dynamical pathways (Fig. 8).

Our analysis is grounded in a causal network framework (Fig. 1a), which summarizes the assumed causal relationships and guides the statistical analysis (Kretschmer et al., 2021). Although mutual information is inherently symmetric, we argue that the chosen temporal resolution and the inclusion of time lags (Fig. 1b) support a causal interpretation. Due to limited sample sizes, we neglect potential linkages between the MJO and the SPV (Barnes et al. 2019). For the seasonal drivers, we adopt a classification based on the winter-mean state, which introduces some information leakage. However, we consider this choice justified in a predictive context, as ENSO and QBO phases are typically well predictable at the beginning of winter. From an operational prediction perspective it is further interesting to consider how the effect of a seasonal driver (which can be seen as a prior for the season) is changed when

knowledge becomes available of a subseasonal driver. This is relevant for emerging seamless prediction systems in which longer-term forecasts are updated with shorter-term ones to address a range of climate-sensitive decisions (Goddard et al. 2014).

Here, we restrict our analysis to commonly used definitions of teleconnection states and extreme events to balance robustness and sample size. We note that our effect estimates will be sensitive to how teleconnection drivers are defined, including the choice of spatial domains and categorical thresholds, as is the case for all measures of association. For example, representing the QBO with only two phases (westerly and easterly) ensures sufficiently large sample sizes but neglects its vertical structure and associated dynamical differences (Shen et al. 2025). Optimizing such choices to maximize signal strength constitutes a separate line of research (DelSole and Tippett 2007). In addition, we acknowledge the growing body of work on learning (causal) representations of teleconnection drivers directly from data as an important research direction, which may yield more tailored and informative driver definitions for specific target variables (Bommer et al. 2025; Kretschmer et al. 2017; Spuler et al. 2025).

Our analysis focuses on the observational record, using ERA5 reanalysis data. Future work should extend this framework to assess the representation of teleconnections in S2S prediction systems and climate models, both as a diagnostic and as a tool to identify windows of opportunity for enhanced predictability. The proposed diagnostics are particularly well suited to this purpose, as they enable rapid and flexible comparisons of teleconnection strength across multiple dimensions. Depending on the application, different aspects can be emphasized, such as the overall teleconnection strength (Fig. 3), the spatial relevance of teleconnections for specific extremes (Figs. 4–6), or variability across timescales (Fig. 7).

The framework thus complements approaches such as the “Sensitivities To the Remote Influence of Periodic Event (STRIPES)” method (Jenney et al. 2019), which relies on periodic behaviour in the variables considered. It can also be combined with “forensic” frameworks to assess teleconnection representations in climate models, providing a nonlinear estimate of causal effects (Shen et al. 2024).

Overall, we argue that combining information theory with causal reasoning provides a powerful and generalizable framework to quantify the strength of teleconnection signals. This approach condenses the multivariate information content of categorical variables in a single interpretable metric, while allowing decomposition into individual contributions and user-defined sets of predictors and target variables. By bridging physics-guided causal inference and data-driven information theory, our study advances a more systematic quantification of teleconnection influences and their relevance for extreme-event predictability on subseasonal to seasonal timescales.

Acknowledgments/Funding

M.K., F.R.S., M.D. and A.W. acknowledge funding from the Horizon Europe project EXPECT (Towards an Integrated Capability to Explain and Predict Regional Climate Changes), Grant

Agreement No. 101137656. M.K. and T.G.S. further acknowledge XAIDA (eXtreme events: Artificial Intelligence for Detection and Attribution), funded through the European Union's Horizon 2020 research and innovation programme under Grant Agreement No. 101003469.

Data and Code availability

The ERA5 reanalysis data is available at the Copernicus Climate Data Store (https://cds.climate.copernicus.eu/). The code will be released on github for the accepted version of the manuscript.

Conflict of interest

Co-author Antje Weisheimer is an editor of QJRMS.

Author contributions

M.K., F.R.S., and L.P. processed the data, and M.K and F.R.S. analysed the data. M.K. led the writing and design of the study. All authors contributed to the writing and the interpretation of results.

References

Afargan-Gerstman, Hilla, Dominik Büeler, C. Ole Wulff, Michael Sprenger, and Daniela I. V. Domeisen. 2024. “Stratospheric Influence on the Winter North Atlantic Storm Track in Subseasonal Reforecasts.” *Weather and Climate Dynamics* 5 (1): 231–49. https://doi.org/10.5194/wcd-5-231-2024.

Albers, John R., and Matthew Newman. 2019. “A Priori Identification of Skillful Extratropical Subseasonal Forecasts.” *Geophysical Research Letters* 46 (21): 12527–36. https://doi.org/10.1029/2019GL085270.

Anstey, James A., Scott M. Osprey, Joan Alexander, et al. 2022. “Impacts, Processes and Projections of the Quasi-Biennial Oscillation.” *Nature Reviews Earth & Environment* 3 (9): 588–603. https://doi.org/10.1038/s43017-022-00323-7.

Ayarzagüena, B., D. Barriopedro, J. M. Garrido-Perez, et al. 2018. “Stratospheric Connection to the Abrupt End of the 2016/2017 Iberian Drought.” *Geophysical Research Letters* 45 (22): 12,639-12,646. https://doi.org/10.1029/2018GL079802.

Baldwin, Mark P., and Timothy J. Dunkerton. 2001. “Stratospheric Harbingers of Anomalous Weather Regimes.” *Science* 294 (5542): 581–84. https://doi.org/10.1126/science.1063315.

Barnes, Elizabeth A., Savini M. Samarasinghe, Imme Ebert-Uphoff, and Jason C. Furtado. 2019. “Tropospheric and Stratospheric Causal Pathways Between the MJO and NAO.” *Journal of Geophysical Research: Atmospheres* 124 (16): 9356–71. https://doi.org/10.1029/2019JD031024.

Bommer, Philine L., Marlene Kretschmer, Fiona R. Spuler, Kirill Bykov, and Marina M. C. Höhne. 2025. “Deep Learning Meets Teleconnections: Improving S2S Predictions for European Winter Weather.” *Machine Learning: Earth* 1 (1): 015002. https://doi.org/10.1088/3049-4753/ade9c2.

Brönnimann, S. 2007. “Impact of El Niño–Southern Oscillation on European Climate.” *Reviews of Geophysics* 45 (3). https://doi.org/10.1029/2006RG000199.

Carvalho-Oliveira, Julianna, Giorgia Di Capua, Leonard F. Borchert, Reik V. Donner, and Johanna Baehr. 2024. “Causal Relationships and Predictability of the Summer East Atlantic Teleconnection.” *Weather and Climate Dynamics* 5 (4): 1561–78. https://doi.org/10.5194/wcd-5-1561-2024.

Cassou, Christophe. 2008. “Intraseasonal Interaction between the Madden–Julian Oscillation and the North Atlantic Oscillation.” *Nature* 455 (7212): 523–27. https://doi.org/10.1038/nature07286.

Chaqdid, Abdelaziz, Alexandre Tuel, Abdelouahad El Fatimy, and Nabil El Moçayd. 2023. “Extreme Rainfall Events in Morocco: Spatial Dependence and Climate Drivers.” *Weather and Climate Extremes* 40 (June): 100556. https://doi.org/10.1016/j.wace.2023.100556.

Charlton-Perez, Andrew J., Wan Ting Katty Huang, and Simon H. Lee. 2021. “Impact of Sudden Stratospheric Warmings on United Kingdom Mortality.” *Atmospheric Science Letters* 22 (2): e1013. https://doi.org/10.1002/asl.1013.

Cosford, Lara R., Rohit Ghosh, Marlene Kretschmer, Clare Oatley, and Theodore G. Shepherd. 2025. “Estimating the Contribution of Arctic Sea-Ice Loss to Central Asia

Temperature Anomalies: The Case of Winter 2020/2021." *Environmental Research Letters* 20 (3): 034007. https://doi.org/10.1088/1748-9326/adae22.

DelSole, Timothy. 2004. *Predictability and Information Theory. Part I: Measures of Predictability*. Journal of the Atmospheric Sciences. October 1. https://journals.ametsoc.org/view/journals/atsc/61/20/1520-0469_2004_061_2425_paitpi_2.0.co_2.xml.

DelSole, Timothy, and Michael K. Tippett. 2007. "Predictability: Recent Insights from Information Theory." *Reviews of Geophysics* 45 (4). https://doi.org/10.1029/2006RG000202.

Di Capua, G., M. Kretschmer, J. Runge, et al. 2019. "Long-Lead Statistical Forecasts of the Indian Summer Monsoon Rainfall Based on Causal Precursors." *Weather and Forecasting* 34 (5): 1377–94. https://doi.org/10.1175/WAF-D-19-0002.1.

Di Capua, G., E. Tyrlis, D. Matei, and R. V. Donner. 2024. "Tropical and Mid-Latitude Causal Drivers of the Eastern Mediterranean Etesians during Boreal Summer." *Climate Dynamics* 62 (10): 9565–85. https://doi.org/10.1007/s00382-024-07411-y.

Domeisen, Daniela I. V., and Amy H. Butler. 2020. "Stratospheric Drivers of Extreme Events at the Earth's Surface." *Communications Earth & Environment* 1 (1): 59. https://doi.org/10.1038/s43247-020-00060-z.

Domeisen, Daniela I. V., Chaim I. Garfinkel, and Amy H. Butler. 2019. "The Teleconnection of El Niño Southern Oscillation to the Stratosphere." *Reviews of Geophysics* 57 (1): 5–47. https://doi.org/10.1029/2018RG000596.

Domeisen, Daniela I. V., Christian M. Grams, and Lukas Papritz. 2020. "The Role of North Atlantic–European Weather Regimes in the Surface Impact of Sudden Stratospheric Warming Events." *Weather and Climate Dynamics* 1 (2): 373–88. https://doi.org/10.5194/wcd-1-373-2020.

Ebert-Uphoff, Imme. 2007. *Measuring Connection Strengths and Link Strengths in Discrete Bayesian Networks*. January 29. http://hdl.handle.net/1853/14331.

Ebert-Uphoff, Imme, and Yi Deng. 2012. "Causal Discovery for Climate Research Using Graphical Models." *Journal of Climate* 25 (17): 5648–65. https://doi.org/10.1175/JCLI-D-11-00387.1.

Elsbury, Dillon, Amy Butler, Yannick Peings, and Gudrun Magnusdottir. 2024. "Sensitivity of Easterly QBO's Boreal Winter Teleconnections and Surface Impacts to SSWs." Journal of Climate. *Journal of Climate* 37 (14): 3675–88. https://doi.org/10.1175/JCLI-D-23-0395.1.

Elsbury, Dillon, Federico Serva, Julie M. Caron, et al. 2026. "QBOi El Niño Southern Oscillation Experiments: Assessing Relationships between ENSO, MJO, and QBO." *Weather and Climate Dynamics* 7 (1): 317–39. https://doi.org/10.5194/wcd-7-317-2026.

Goddard, Lisa, Walter E. Baethgen, Haresh Bhojwani, and Andrew W. Robertson. 2014. "The International Research Institute for Climate & Society: Why, What and How." *Earth Perspectives* 1 (1): 10. https://doi.org/10.1186/2194-6434-1-10.

Hamed, Raed, Sem Vijverberg, Anne F. Van Loon, Jeroen Aerts, and Dim Coumou. 2023. "Persistent La Niñas Drive Joint Soybean Harvest Failures in North and South America." *Earth System Dynamics* 14 (1): 255–72. https://doi.org/10.5194/esd-14-255-2023.

Holton, James R., and Hsiu-Chi Tan. 1980. “The Influence of the Equatorial Quasi-Biennial Oscillation on the Global Circulation at 50 Mb.” Journal of the Atmospheric Sciences. *Journal of the Atmospheric Sciences* 37 (10): 2200–2208. https://doi.org/10.1175/1520-0469(1980)037%3C2200:TIOTEQ%3E2.0.CO;2.

Jenney, A. M., D. A. Randall, and E. A. Barnes. 2019. “Quantifying Regional Sensitivities to Periodic Events: Application to the MJO.” *Journal of Geophysical Research: Atmospheres* 124 (7): 3671–83. https://doi.org/10.1029/2018JD029457.

Karpechko, Alexey Yu., Peter Hitchcock, Dieter H. W. Peters, and Andrea Schneidereit. 2017. “Predictability of Downward Propagation of Major Sudden Stratospheric Warmings.” *Quarterly Journal of the Royal Meteorological Society* 143 (704): 1459–70. https://doi.org/10.1002/qj.3017.

Kraskov, Alexander, Harald Stögbauer, and Peter Grassberger. 2004. “Estimating Mutual Information.” *Physical Review E* 69 (6): 066138. https://doi.org/10.1103/PhysRevE.69.066138.

Kretschmer, Marlene, Samantha V. Adams, Alberto Arribas, et al. 2021. “Quantifying Causal Pathways of Teleconnections.” *Bulletin of the American Meteorological Society* 102 (12): E2247–63. https://doi.org/10.1175/BAMS-D-20-0117.1.

Kretschmer, Marlene, Dim Coumou, Laurie Agel, Mathew Barlow, Eli Tziperman, and Judah Cohen. 2018. “More-Persistent Weak Stratospheric Polar Vortex States Linked to Cold Extremes.” Bulletin of the American Meteorological Society. *Bulletin of the American Meteorological Society* 99 (1): 49–60. https://doi.org/10.1175/BAMS-D-16-0259.1.

Kretschmer, Marlene, Jakob Runge, and Dim Coumou. 2017. “Early Prediction of Extreme Stratospheric Polar Vortex States Based on Causal Precursors.” *Geophysical Research Letters* 44 (16): 8592–600. https://doi.org/10.1002/2017GL074696.

Kretschmer, Marlene, Giuseppe Zappa, and Theodore G. Shepherd. 2020. “The Role of Barents–Kara Sea Ice Loss in Projected Polar Vortex Changes.” *Weather and Climate Dynamics* 1 (2): 715–30. https://doi.org/10.5194/wcd-1-715-2020.

Kumar, Vinay, Shigeo Yoden, and Matthew H. Hitchman. 2022. “QBO and ENSO Effects on the Mean Meridional Circulation, Polar Vortex, Subtropical Westerly Jets, and Wave Patterns During Boreal Winter.” *Journal of Geophysical Research: Atmospheres* 127 (15): e2022JD036691. https://doi.org/10.1029/2022JD036691.

Lauritzen, S. L., and D. J. Spiegelhalter. 1988. “Local Computations with Probabilities on Graphical Structures and Their Application to Expert Systems.” *Journal of the Royal Statistical Society Series B: Statistical Methodology* 50 (2): 157–94. https://doi.org/10.1111/j.2517-6161.1988.tb01721.x.

Lee, R. W., S. J. Woolnough, A. J. Charlton-Perez, and F. Vitart. 2019. “ENSO Modulation of MJO Teleconnections to the North Atlantic and Europe.” *Geophysical Research Letters* 46 (22): 13535–45. https://doi.org/10.1029/2019GL084683.

Leung, Lai-Yung, and Gerald R. North. 1990. “Information Theory and Climate Prediction.” Journal of Climate. *Journal of Climate* 3 (1): 5–14. https://doi.org/10.1175/1520-0442(1990)003%3C0005:ITACP%3E2.0.CO;2.

Ma, Tianjiao, Wen Chen, Xiadong An, Chaim I. Garfinkel, and Qingyu Cai. 2023. “Nonlinear Effects of the Stratospheric Quasi-Biennial Oscillation and ENSO on the North Atlantic Winter

Atmospheric Circulation." *Journal of Geophysical Research: Atmospheres* 128 (17): e2023JD039537. https://doi.org/10.1029/2023JD039537.

Mariotti, Annarita, Cory Baggett, Elizabeth A. Barnes, et al. 2020. "Windows of Opportunity for Skillful Forecasts Subseasonal to Seasonal and Beyond." Bulletin of the American Meteorological Society. *Bulletin of the American Meteorological Society* 101 (5): E608–25. https://doi.org/10.1175/BAMS-D-18-0326.1.

Mastere, Mohamed, Roumaissae Azguet, Soufiana Mekouar, et al. 2025. "Managing Disaster Risks in Moroccan Cities: Perceptions and Preparedness with Insights from the Rabat Region." *International Journal of Disaster Risk Reduction* 128 (October): 105739. https://doi.org/10.1016/j.ijdrr.2025.105739.

Mindlin, Julia, Theodore G. Shepherd, Marisol Osman, Carolina S. Vera, and Marlene Kretschmer. 2025. "Explaining and Predicting the Southern Hemisphere Eddy-Driven Jet." *Proceedings of the National Academy of Sciences* 122 (29): e2500697122. https://doi.org/10.1073/pnas.2500697122.

Monnin, Erika, Marlene Kretschmer, and Inna Polichtchouk. 2022. "The Role of the Timing of Sudden Stratospheric Warmings for Precipitation and Temperature Anomalies in Europe." *International Journal of Climatology* 42 (6): 3448–62. https://doi.org/10.1002/joc.7426.

Osman, Marisol, Theodore G. Shepherd, and Carolina S. Vera. 2022. "The Combined Influence of the Stratospheric Polar Vortex and ENSO on Zonal Asymmetries in the Southern Hemisphere Upper Tropospheric Circulation during Austral Spring and Summer." *Climate Dynamics* 59 (9–10): 2949–64. https://doi.org/10.1007/s00382-022-06225-0.

Pearl, Judea. 1988. *Probabilistic Reasoning in Intelligent Systems*. Elsevier. https://doi.org/10.1016/C2009-0-27609-4.

Pearl, Judea. 2009. *Causality: Models, Reasoning, and Inference*. 2nd ed. Cambridge University Press. https://doi.org/10.1017/CBO9780511803161.

Pearl, Judea. 2013. "Understanding Simpson's Paradox." *SSRN Electronic Journal*, ahead of print. https://doi.org/10.2139/ssrn.2343788.

Roberts, Christopher D., Magdalena A. Balmaseda, Laura Ferranti, and Frederic Vitart. 2023. "Euro-Atlantic Weather Regimes and Their Modulation by Tropospheric and Stratospheric Teleconnection Pathways in ECMWF Reforecasts." Monthly Weather Review. *Monthly Weather Review* 151 (10): 2779–99. https://doi.org/10.1175/MWR-D-22-0346.1.

Rouges, Emmanuel, Marlene Kretschmer, and Theodore G. Shepherd. 2025. "On the Link Between Weather Regimes and Energy Shortfall During Winter for 28 European Countries." *Meteorological Applications* 32 (4): e70077. https://doi.org/10.1002/met.70077.

Runge, Jakob, Jobst Heitzig, Norbert Marwan, and Jürgen Kurths. 2012. "Quantifying Causal Coupling Strength: A Lag-Specific Measure for Multivariate Time Series Related to Transfer Entropy." *Physical Review E* 86 (6): 061121. https://doi.org/10.1103/PhysRevE.86.061121.

Saggioro, Elena, Theodore G. Shepherd, and Jeff Knight. 2024. "Probabilistic Causal Network Modelling of Southern Hemisphere Jet Sub-Seasonal to Seasonal Predictability." Journal of Climate. *Journal of Climate* 1 (aop). https://doi.org/10.1175/JCLI-D-23-0425.1.

Shen, Xiaocen, Marlene Kretschmer, and Theodore G. Shepherd. 2024. "A Forensic Investigation of Climate Model Biases in Teleconnections: The Case of the Relationship

Between ENSO and the Northern Stratospheric Polar Vortex." *Journal of Geophysical Research: Atmospheres* 129 (19): e2024JD041252. https://doi.org/10.1029/2024JD041252.

Son, Seok-Woo, Yuna Lim, Changhyun Yoo, Harry H. Hendon, and Joowan Kim. 2017. "Stratospheric Control of the Madden–Julian Oscillation." Journal of Climate. *Journal of Climate* 30 (6): 1909–22. https://doi.org/10.1175/JCLI-D-16-0620.1.

Specq, Damien, and Lauriane Batté. 2022. "Do Subseasonal Forecasts Take Advantage of Madden–Julian Oscillation Windows of Opportunity?" *Atmospheric Science Letters* 23 (4): e1078. https://doi.org/10.1002/asl.1078.

Spuler, Fiona R., Marlene Kretschmer, Magdalena Alonso Balmaseda, Yevgeniya Kovalchuk, and Theodore G. Shepherd. 2025. "Learning Predictable and Informative Dynamical Drivers of Extreme Precipitation Using Variational Autoencoders." *Weather and Climate Dynamics* 6 (3): 995–1014. https://doi.org/10.5194/wcd-6-995-2025.

Spuler, Fiona R., Marlene Kretschmer, Yevgeniya Kovalchuk, Magdalena Alonso Balmaseda, and Theodore G. Shepherd. 2024. "Identifying Probabilistic Weather Regimes Targeted to a Local-Scale Impact Variable." *Environmental Data Science* 3 (January): e25. https://doi.org/10.1017/eds.2024.29.

Vitart, Frédéric, and Andrew W. Robertson. 2018. "The Sub-Seasonal to Seasonal Prediction Project (S2S) and the Prediction of Extreme Events." *Npj Climate and Atmospheric Science* 1 (1): 3. https://doi.org/10.1038/s41612-018-0013-0.

Wang, Haoxiang, Jian Rao, Dong Guo, Yimin Liu, and Yixiong Lu. 2025. "Limited Nonlinearity of Joint ENSO–QBO Effects from the Stratosphere to the Troposphere." *Atmospheric and Oceanic Science Letters*, August 18, 100704. https://doi.org/10.1016/j.aosl.2025.100704.

Weisheimer, Antje, Damien Decremer, David MacLeod, et al. 2019. "How Confident Are Predictability Estimates of the Winter North Atlantic Oscillation?" *Quarterly Journal of the Royal Meteorological Society* 145 (S1): 140–59. https://doi.org/10.1002/qj.3446.

Wheeler, Matthew C., and Harry H. Hendon. 2004. "An All-Season Real-Time Multivariate MJO Index: Development of an Index for Monitoring and Prediction." Monthly Weather Review. *Monthly Weather Review* 132 (8): 1917–32. https://doi.org/10.1175/1520-0493(2004)132%3C1917:AARMMI%3E2.0.CO;2.

Yamazaki, Koji, Tetsu Nakamura, Jinro Ukita, and Kazuhira Hoshi. 2020. "A Tropospheric Pathway of the Stratospheric Quasi-Biennial Oscillation (QBO) Impact on the Boreal Winter Polar Vortex." *Atmospheric Chemistry and Physics* 20 (8): 5111–27. https://doi.org/10.5194/acp-20-5111-2020.

Zhang, Chidong, and Bosong Zhang. 2018. "QBO-MJO Connection." *Journal of Geophysical Research: Atmospheres* 123 (6): 2957–67. https://doi.org/10.1002/2017JD028171.